The growth of orogenic belts and the role of crustal heterogeneities in decollement tectonics

Dennis L. Harry *Department of Geology, University of Alabama, Box 870338, Tuscaloosa, Alabama 35487-0338*
John S. Oldow, **Dale S. Sawyer** *Department of Geology and Geophysics, Rice University, P.O. Box 1892, Houston, Texas 77251*

ABSTRACT

A series of finite element models of contractional deformation are presented that examine the role preexisting mechanical heterogeneities within the lithosphere play in controlling the partitioning of stress and strain during orogenesis. The models focus particularly on orogens that develop near previously rifted continental margins, although many of the observations are relevant to other fold and thrust belts. The models indicate that orogen evolution is strongly influenced by crustal architecture during the first 150 to 200 km of shortening. Major decollements develop at midcrustal and lower crustal levels, partitioning strain into upper crustal, lower crustal, and mantle strain domains. The magnitude and spatial distribution of strain within each domain are nearly uniform but differ significantly between domains. The decollements extend throughout the entire width of the orogen, providing a successively increasing degree of decoupling between deformation in the shallow crust and deeper levels. The midcrustal decollement terminates beneath the leading edge of the thrust front, but the deep crustal decollement extends more than 500 km beyond the foreland. This allows up to 5%–10% strain to develop well in front of the orogenic belt. In the interior of the orogen, deformation extends through all levels of the crust beginning during the earliest stages of contraction. Deformation propagates continentward with increasing shortening, with the foreland regions undergoing the most intense shortening in the shallow crust. The loci of maximum total shortening within the upper and lower crust are laterally offset, with the thickest crust lying continentward of the greatest elevations and the site of most intense surface deformation. This pattern of crustal thickness variation is a primary feature of orogenesis in the models and is not related to postorogenic collapse. After 150 to 200 km of shortening, sufficient topography develops to cause the balance between rock strength, gravitational forces, and shear stress on the basal detachment to dominate the style of deformation. Preexisting mechanical heterogeneities thereafter exert little influence on orogenic processes.

INTRODUCTION

The manner in which stress and strain are partitioned within the lithosphere during contractional deformation has received little quantitative attention, in spite of recent observations that indicate that such partitioning is a fundamental aspect of orogenesis. Models based on surface geological relations and deep-crustal seismic studies suggest a pattern of vertical strain partitioning in which crustal imbricates are decoupled from the lower crust or upper mantle by a basal decollement system (e.g., Laubscher, 1983; Cook, 1984; Roeder, 1989; Oldow et al., 1990). The manner in which strain is partitioned varies horizontally, with deformation in the crust extending to greater depths beneath the hinterland than beneath the foreland. This assertion of large-scale partitioning of strain within the crust focuses attention on several poorly constrained aspects of the development of orogenic belts. These include the depth and character of deformation beneath hinterland regions, the degree to which deformation in the orogen is coupled to processes within the deep lithosphere, and mechanisms for relaying compressive stress through the hinterland and into the foreland.

Seismic reflection surveys in foreland fold and thrust belts have documented basal decollement systems that typically dip shallowly toward the hinterland of the orogen (e.g., Bally et al., 1966; Cook et al., 1979; Potter et al., 1986; Luetgert et al., 1987; Pratt et al., 1988; Sheridan et al., 1991). Continuity of foreland decollements beneath the hinterland is less clear but has been inferred from deep crustal seismic reflection surveys in the Canadian Rockies, Brooks Range, Appalachians, Pyrenees, and Alps (Cook et al., 1991; Levander et al., in press; Costain et al., 1989; Choukroune et al., 1989; Pfiffner et al., 1990). Seismic reflection data have been combined with geometric and mass balance arguments in the proposition that orogenic belts are underlain by a throughgoing decollement system (Oldow et al., 1990). In this view, complex crustal structures are linked by the underlying decollement and separated from the underlying lower crust and upper mantle. Geologic observations currently offer no conclusive evidence for or against large-scale vertical partitioning of strain within contractional belts. Some workers argue against a throughgoing decollement system and propose that basal foreland thrusts root beneath the hinterland (e.g., Miller and Gans, 1989). In this view, foreland shortening is accommodated within the hinterland by homogeneous contraction extending to great depth, thus removing the necessity of decoupling the crust from the underlying mantle.

A primary difficulty in distinguishing between vertical strain partitioning and homogeneous shortening in the internides of orogenic belts is that many of the diagnostic predictions of both models center around processes occurring in the lower crust and upper

Data Repository item 9555 contains additional material related to this article.

GSA Bulletin; December 1995; v. 107; no. 12; p. 1411–1426; 14 figures; 1 table.

mantle. These regions are poorly understood, due to limited geological and geophysical observations. This paper presents a series of dynamic models of contractional deformation that examine the spatial and temporal partitioning of strain. In particular, we focus on the role that preexisting mechanical heterogeneities play in determining the manner in which strain is partitioned laterally and with depth and how partitioning varies during progressive shortening. The models are necessarily simplistic and do not consider important plate boundary processes such as oblique convergence, traction at the base of the lithosphere, and along-strike components of displacement. These processes undoubtedly play a major role in governing the evolution of convergent orogens, as has been shown in previous studies (e.g., Braun, 1993; Beaumont and Quinlan, 1994; Nicholson et al., 1994). However, the previous studies did not consider the effect that preexisting heterogeneities within the lithosphere have on orogen development.

The models presented here are relevant to orogens that developed during contractional deformation at previously rifted continental margins. Examples of such orogens include the Alaskan Brooks Range, the Ouachita orogen, the southern Appalachians, and the Mesozoic western Cordillera of North America (Oldow et al., 1989; Rankin et al., 1989; Viele and Thomas, 1989). Mechanical heterogeneities that may have influenced the style of contractional deformation in these orogenic belts result from seaward thinning of the continental crust at the rifted margin, the boundary between weak continental lithosphere and strong oceanic lithosphere, and the presence of thick sedimentary accumulations on the continental shelf. The models indicate that partitioning of strain into shallow (thin-skinned) deformation in the foreland and deep-seated deformation in the hinterland may be accommodated by the development of subhorizontal shear zones in the middle and lower crust that extend beneath the entire width of the orogen. Lateral growth of these shear zones during shortening results in migration of the leading edge of the foreland toward the continent and progressive propagation of deformation to deeper levels of the crust in the proximal foreland. Partitioning of strain into deep-seated deformation in the internides and shallow deformation in the foreland and the progressive growth of deformation both outward and downward with time have previously been proposed to explain the evolution of many orogenic belts (e.g., Bally et al., 1966; Bally, 1981).

PHYSICAL MODELS OF MOUNTAIN BUILDING

The morphologic evolution of foreland fold and thrust belts has been described as broadly analogous to the growth of a critically tapered wedge of homogeneous plastic material overlying a frictional basal decollement (Chapple, 1978; Dahlen, 1984). The morphology of the fold and thrust belt is controlled by the balance between the work required to produce slip on the basal decollement, the gravitational work required to produce uplift of the material within the wedge, and frictional work required to deform the wedge (Dahlen and Barr, 1989). This balance occurs at a critical topographic slope, which is determined by the cohesiveness of the rocks within the orogen and the strength of the basal decollement. The slope of the wedge remains constant throughout the orogenic episode unless the rate of material accretion or the rate of denudation changes. Thus, during the early stages of orogenesis (when the rate of accretion is assumed to exceed the rate of denudation) the foreland belt widens as the elevation in the hinterland increases. The critically tapered wedge model accounts for forelandward propagation of deformation and is compatible with the gross morphologic and thermal evolution of the foreland in many contractional belts (Dahlen and Barr, 1989; Barr and Dahlen, 1989; Barr et al., 1991).

A difficulty of the critically tapered wedge model is the assumption of uniform plasticity. The continental lithosphere is rheologically stratified, and its strength at any given depth depends upon composition, temperature, and strain rate (Carter and Tsenn, 1987; Ranalli and Murphy, 1987). The effects of rheologic stratification on the evolution of marginal orogens have been examined by approximating the lithosphere as a thin viscous sheet, with the viscosity given by the integrated strength of the lithosphere (England and McKenzie, 1982; England et al., 1985; Houseman and England, 1986). Thin sheet models indicate that the strength of the uppermost mantle (primarily determined by its temperature) plays a critical role in determining the rate, duration, and style of deformation (England and McKenzie, 1982; Houseman and England, 1986).

The thin sheet models do not directly examine changing patterns of vertical stress and strain partitioning within the lithosphere during contraction. Several quantitative studies have demonstrated that complex spatial and temporal patterns of strain partitioning can result if deformation in the crust is partially coupled with deformation in the mantle (Bott, 1990; Wdowonski and O'Connell, 1991). Traction applied at the base of the crust by subducting mantle may produce conjugate dipping shear zones that serve as oppositely facing detachments in convergent orogens (Willett et al., 1993, Beaumont and Quinlan, 1994). The shear stress on these detachments transmits strain into the upper crust and induces shallow deformation. However, these models do not consider the impact that preexisting lateral strength variations have on orogen evolution. Chery et al. (1991) noted that lithospheric heterogeneities produced during previous extensional episodes have a profound effect on subsequent contractional deformation. This is the focus of the modeling studies described below.

MODELING CONTRACTIONAL DEFORMATION IN THE CONTINENTAL LITHOSPHERE

Contraction is modeled using the finite element method described by Dunbar (1988), which has previously been used to study deformation and magmatism in extensional regimes (Dunbar and Sawyer, 1989; Sawyer and Harry, 1991; Harry and Sawyer, 1992a, 1992b; Harry et al., 1993). The method is adapted from the algorithm of Zienkiewicz and Godbole (1975) and solves for strain rate and temperature according to the plane strain equations governing viscoplastic flow and the two-dimensional heat equation (including heat generation in the continental crust). Body forces are included and area is conserved within each element in the mesh. A time-stepping technique is used in which the mechanical problem is solved first, determining the strain rate at each node in the finite element mesh. The nodal positions are then stepped forward in time, and the heat equation is solved to determine the temperature within the model at the new time. The key features of the model are as follows: (1) the strength of the model lithosphere is temperature, composition, and strain rate dependent and varies both laterally and with depth, and (2) lateral variations in mass are regionally compensated, with supporting stresses distributed by the shear strength of the lithosphere according to the ductile flow relations. Although the model does not include elasticity, the ability of the model to sustain shear stress results in a flexural style of isostatic compensation (e.g., DeBremaecker, 1977).

TABLE 1. PHYSICAL PARAMETERS USED IN THE MODELING STUDY

Thermal properties *				
Surface heat flux (continent)	55×10^{-3} W m^{-2}			
Mantle heat flux (continent)	29×10^{-3} W m^{-2}			
Surface heat production (continent)	3×10^{-6} W m^{-3}			
Thermal decay depth (continent)	10 km			
Thermal expansion coefficient	3.1×10^{-5} °K^{-1}			
Crust conductivity	2.5 W m^{-1} °K^{-1}			
Mantle conductivity	3.4 W m^{-1} °K^{-1}			
Sediment specific heat	800 J kg^{-1} °K^{-1}			
Continental crust specific heat	875 J kg^{-1} °K^{-1}			
Oceanic crust specific heat	875 J kg^{-1} °K^{-1}			
Mantle specific heat	1250 J kg^{-1} °K^{-1}			
Rheologic Properties†				
	log10 A (MPa^{-n} s^{-1})	Qc (Kj mole^{-1})	n	ρ (kg m^{-3})
Sediments: Solnhofen limestone§	4.3	213	1.7	2650
Continental crust: Quartz diorite#	-2.9	219	2.4	2850
Oceanic crust: Stillwater gabbro**	9.7	497	3.4	2900
Mantle: Wet Aheim dunite††	2.6	498	4.5	3300

*Heat production at depth z is given by $a_0\exp\{-zd\}$, where a_0 is the surface heat production and d is the thermal decay depth. The choice of thermal parameters is based on Sclater et al. (1980).

†Strain rate is given by $A\sigma^n\exp\{Qc/RT\}$, where σ is stress, R is the universal gas constant, and T is temperature.

§Schmid et al. (1977).

#Hansen and Carter (1982).

**Wilks and Carter (1990).

††Chopra and Paterson (1981).

Deformation within each element of the mesh is governed by the empirical power-law creep relation for the selected rock type (Table 1), with the maximum stress limited by Byerlee's (1968, 1978) frictional relation:

$$\sigma_y = 60 \text{ MPa} + 0.6(P_L - P_p) \quad (1)$$

where P_p is pore pressure and P_L is lithostatic pressure. Pore pressure was assumed to be $0.55P_L$. The boundary conditions (Fig. 1) include constant velocities on the sides of the model, constant temperature at the surface, and constant heat flux through the base of the model (the thermal parameters of the model are shown in Table 1). The constant heat flux condition at the base of the model allows the lower mechanical lithosphere to become warmer during contraction. The duration of contraction at most orogens is at least as long as the lithosphere's characteristic thermal time constant (ca. 60 m.y.), so this condition seems reasonable. At contraction rates and durations typical of orogenic episodes (~1–5 km/m.y.) the model results are not greatly sensitive to the lower thermal boundary condition. Figure 2 compares the results of models using constant heat flux and constant temperature lower boundary conditions. The latter case allows no conductive heating of the lower lithosphere. The thermal state of crust and upper mantle and the net strength of the lithosphere are similar in both models.

The constant velocity boundary condition prescribes no vertical

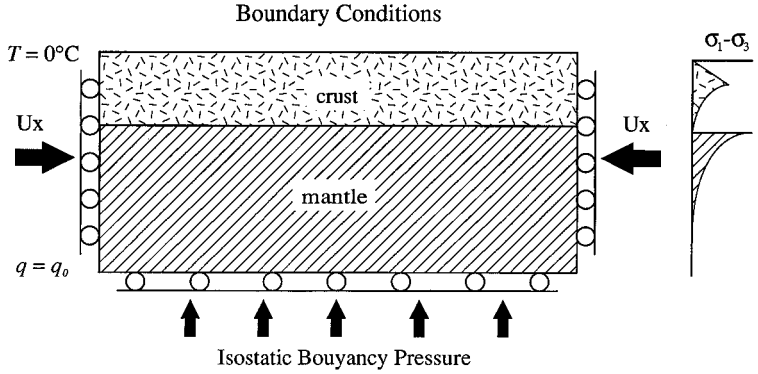

Figure 1. Boundary conditions used in finite element models. The surface of the model is held at a constant temperature of 0 °C and the base of the model is subjected to a constant heat flux, q_a (computed from the steady-state thermal structure of the model prior to contraction). Constant velocity and zero shear stress boundary conditions are applied at one or both sides of the model. The isostatic buoyancy pressure applied to the base of the model is the pressure required to keep the model at the appropriate elevation relative to sea level prior to contraction. T, temperature; q, heat flux; u_x, velocity; σ_1–σ_3, difference in maximum and minimum principal stress.

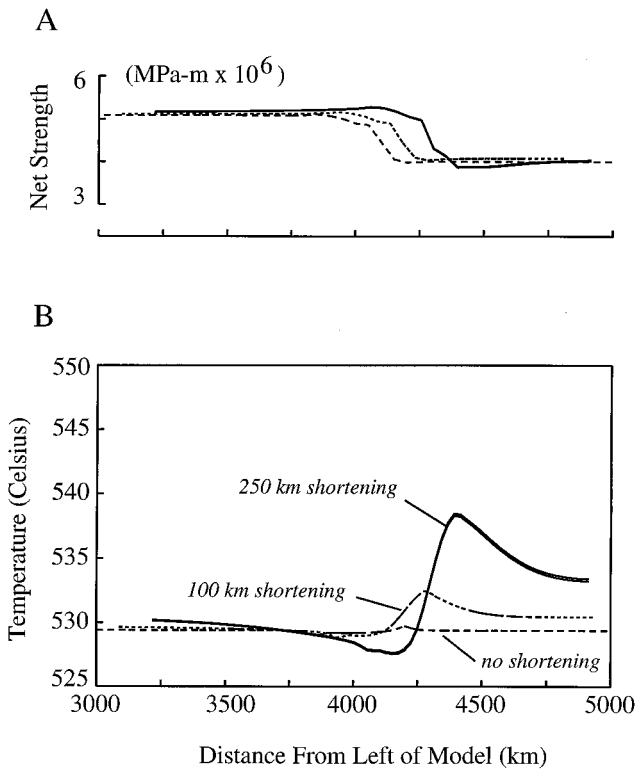

Figure 2. Comparison of model behavior under constant temperature and constant heat flux basal boundary conditions. Results are shown prior to contraction (dashed lines), after 100 km of shortening (dotted lines), and after 250 km of shortening (solid lines). (A) Net strength of the model lithosphere. (B) Temperature at the crust/mantle boundary. The net strength of the lithosphere was obtained by integrating flow stress over the thickness of the model at a constant strain rate of 10^{-15} s^{-1}. The model evolves similarly under either boundary condition, and the curves representing the different boundary conditions are indistinguishable from one another. The model has the same geometry and physical properties as model 3, which is described in detail in the text.

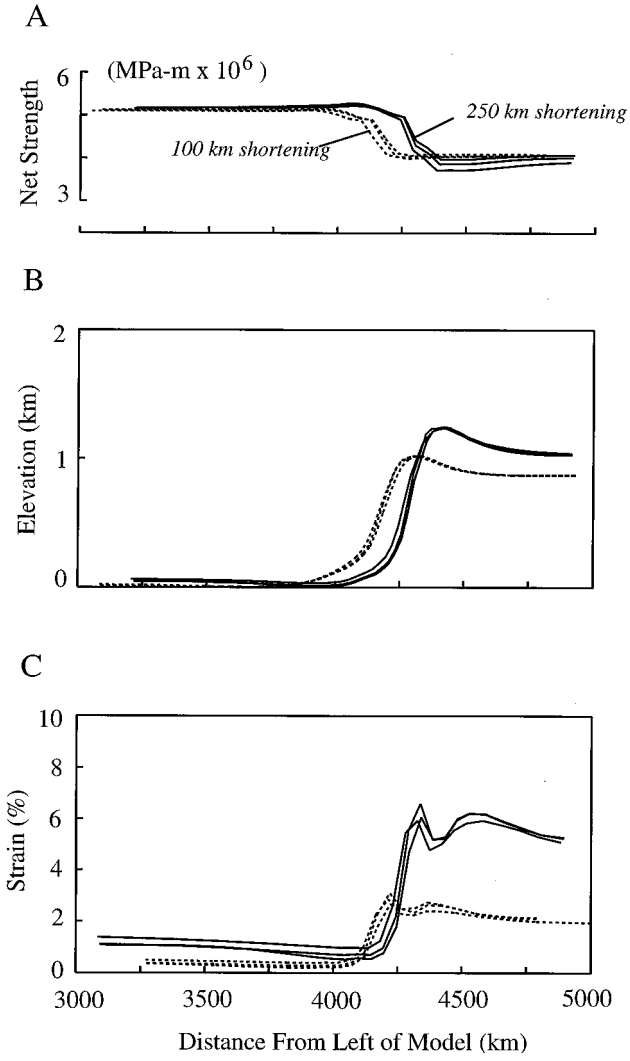

Figure 3. Dependence of model behavior on the constant velocity boundary condition. The results after 100 km and 250 km total shortening are shown for contraction rates of 2.5, 5, and 10 mm/yr. (A) Net strength of the model lithosphere. (B) Surface elevation. (C) Horizontal strain at the top of the mantle. The results of each of the models are similar after equal amounts of shortening.

variations in horizontal displacement at the sides of the model. If there are no lateral variations in strength, then strain is distributed evenly and the model deforms by homogeneous shortening and thickening. The model is not greatly sensitive to modest (factor of two) variations in the rate of contraction (Fig. 3). Thus, the model results depend primarily on the net amount of shortening rather than the duration or rate of contraction and may be extrapolated to faster or slower contraction rates by making the appropriate adjustment in time.

The mechanical boundary conditions used in the models prescribe no shear stress at the sides or base of the model. Therefore, traction at the base of the lithosphere is not modeled. However, subhorizontal shear zones develop in the lower and middle crust in the models as a natural consequence of contraction in a rheologically stratified lithosphere (also see Beaumont and Quinlan, 1994). These shear zones act as basal detachments, transmitting shear stress to the base of the lower crust and upper crust. Nonetheless, it is important to recognize that the models illustrate the effects of crustal strength heterogeneities in isolation from important basal boundary condition effects that are associated with plate subduction. Basal traction is probably a dominant control on many features of orogen evolution, particularly in development of orogen-bounding dipping shear zones during subduction orogeny (e.g., Willett et al., 1993; Beaumont and Quinlan, 1994). The models shown here should illustrate modifying factors that would be superimposed upon the first-order patterns of deformation produced by basal shear during mantle subduction.

RESULTS

The models described below illustrate the manner in which preexisting strength heterogeneities arising from variations in the structure of the lithosphere affect the gross morphological evolution of orogens and the partitioning of stress and strain within orogenic belts. The models are not intended to represent specific geologic

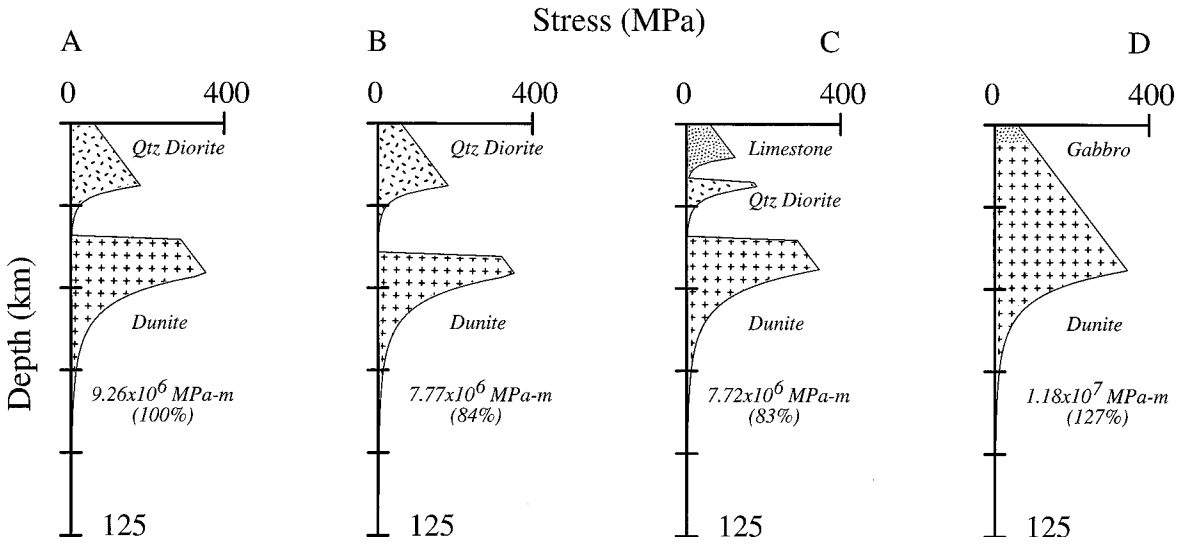

Figure 4. Flow stress in the lithosphere. The thermal parameters are given in Table 1, and the strain rate is 10^{-15} s^{-1}. The net strength of the lithosphere is obtained by integrating the flow stress over the thickness of the lithosphere and is indicated at the bottom of each figure (with comparison to the nominal continental lithosphere). (A) Continental lithosphere with 35-km-thick crust. (B) Continental lithosphere with 40-km-thick crust. (C) Continental lithosphere with 35-km-thick crust, including a 17.5-km-thick sedimentary section. (D) Oceanic lithosphere.

environments in detail but are instead designed to approximate fundamental types of strength heterogeneities that are encountered in orogenic provinces. We examine three important types of mechanically induced heterogeneities.

(1) Variations in the thickness of the continental crust. Regions with thick crust are weaker than adjacent regions because a portion of the strong uppermost mantle has been replaced with weaker crustal material (Figs. 4A and 4B).

(2) Variations in the thickness of the sedimentary section. Thick sedimentary sections (~15 km) such as those found at many rifted continental margins weaken the middle crust by replacing relatively strong crystalline rocks with weaker sedimentary rocks (Fig. 4C).

(3) Juxtaposition of different types of crust. This is most pronounced at the ocean-continent boundary, where strong oceanic lithosphere abuts weaker continental crust (Fig. 4D). The discussion below focuses on results that are fundamental consequences of the rheologic heterogeneities, rather than those which reflect variations in the geometry with which a particular class of heterogeneities is parameterized. For example, we examine the effects that a thick sedimentary section may have on orogenesis, but do not examine in detail the effect that variations in the width of the sedimentary basin or the slope of the crystalline basement may have on the evolution of the orogen.

The models illustrate the evolution of an orogen contracting at a rate of 5 mm/yr, applied as a constant velocity at the left side of the model. This results in 500 km of shortening over a 100 m.y. period. These values are reasonable for many orogens, which typically exhibit several hundred kilometers of shortening over periods ranging from 50 m.y. to 150 m.y. (e.g., the Ouachita, Variscan, Andean, and Sevier orogenies: Viele and Thomas, 1989; Matte, 1991; Allmendinger et al., 1990; Lawton and Trexler, 1991). Recurrent deformation may result in multiple orogenic episodes over periods of several hundred million years, as observed in the western North American Cordillera, the Appalachians, Andean Cordillera, and Variscan belt (James, 1971; Hatcher and Odom, 1980; Oldow et al., 1989; Matte, 1991).

Model 1. Weakness in the Mantle

The first model examines the case in which deformation is focused by a preexisting weakness in the uppermost mantle. This is likely to be the strongest portion of the lithosphere (Fig. 4), so a weakness of this form is expected to have a profound effect on orogen development. For convenience, the weakness is modeled as a 350-km-wide region in which the crust thickens from 35 km to 40 km. This reduces the strength of the lithosphere by up to 30% (Fig. 5). The zero shear stress boundary condition at the left side of the model produces an axis of symmetry, so the results represent the right half of a symmetric model. Deformation in the mantle is concentrated on the left side of the model beneath the thickest crust, where the mantle is weakest. The mantle in this region deforms by pure shear shortening and thickening. A shear zone develops at the base of the crust in this region as the mantle moves to the left relative to the overlying crust (Fig. 5). Shear along this boundary produces a horizontal strain in the crust that is more broadly distributed in the upper crust than in the lower crust (Fig. 6). The loci of maximum strain in the shallow and deep crust are horizontally offset from one another (Fig. 6). At the surface, the locus of greatest horizontal strain lies directly above the contact between the regions of thickened and unthickened crust, whereas at the base of the crust it is located where the crust is thickest (and hence, the mantle is weakest). The offset in the loci of strain at different levels in the crust indicates that strain is transmitted upward through the crust at an angle that dips toward the locus of most intense shortening in the mantle. This dipping pattern of strain within the crust is similar to that produced in the models of Beaumont and Quinlan (1994), who used a shear boundary condition at the base of the crust. The more

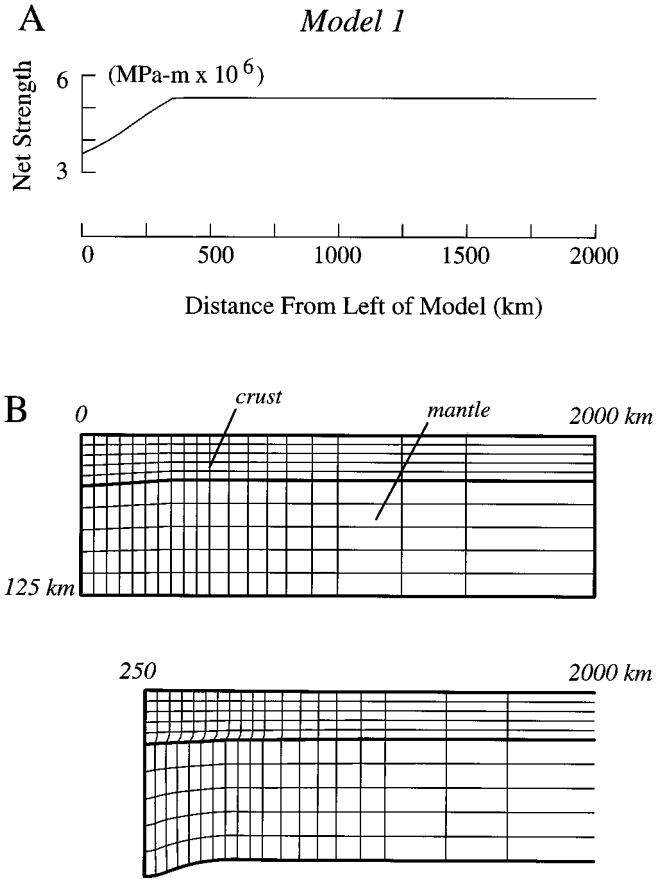

Figure 5. Model 1 (upper mantle weakness); structural features. The weakness on the left side of the model is created by increasing the crustal thickness from 35 km to 40 km over a 350-km-wide region. (A) Lateral variation in the total strength of the lithosphere, obtained by integrating the flow stress over depth. Flow stress was calculated using the model strain rates after the first time step (0.5 m.y. of contraction). (B) Finite element mesh prior to contraction and after 250 km of shortening. The model was 5000 km wide prior to contraction, but only the first 2000 km are shown. Heavy lines indicate lithologic boundaries. Vertical exaggeration is 5:1.

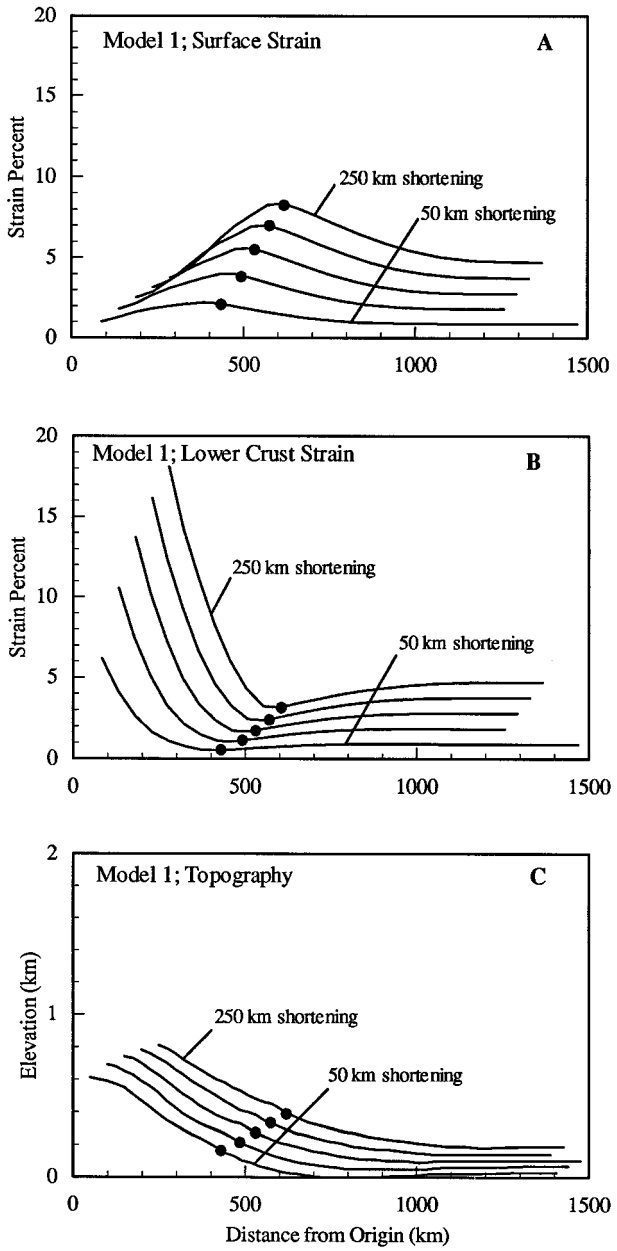

Figure 6. Model 1 (upper mantle weakness); elevation and horizontal strain. Solid circles indicate the position where the crust begins to thicken toward the left. (A) Surface strain is greatest above the position where the crust begins to thicken and decreases monotonically in both directions. (B) Strain at the base of the crust in the weakened region is much more strongly localized and is of higher magnitude than at the surface. (C) Uplift is moderate and is distributed well beyond the weakened region.

focused nature of strain at depth results in much larger maximum values at the base of the crust (18%) than at the surface (9%). A small amount of strain (up to 5%) is transmitted into the unweakened interior of the model, which exhibits similar magnitudes of strain at both the surface and the base of the crust. The variation with depth of the width of the region undergoing strain is evidenced by seismic reflection profiles, which indicate that deformation in foreland regions is generally restricted to the upper 10 to 15 km of the crust (Cook et al., 1979; Potter et al., 1986; Luetgert et al., 1987; Pratt et al., 1988; Allmendinger et al., 1990; Sheridan et al., 1991). Deep-crustal seismic profiling and exposed greenschist to amphibolite facies rocks in the internides of many orogens suggest that contractional deformation within the hinterland extends at least to midcrustal depths (Matte, 1991; Foster et al., 1992; Snyder et al., 1990; Yoos et al., 1991).

Uplift in the model is broadly distributed due to regional isostatic compensation of the thickened crust (Fig. 6C). A nearly constant topographic slope is maintained during shortening, with the width of the orogen (as defined by its topographic expression) increasing as the maximum elevation increases. This is similar to the behavior of a critically tapered wedge of homogeneous material (Elliot, 1976; Dahlen, 1984) and is not surprising as the crust in the model contains no major mechanical heterogeneities. Notably lacking in the model is a well-developed foreland basin topographic low.

This is because crustal thickening during shortening is more localized at depth than at the surface, creating a large crustal root and excess buoyancy within the lithosphere. This results in uplift of the shallow crust rather than subsidence, as would be predicted if crustal thickening were achieved by emplacement of surface topography. The model leads us to speculate that orogens lacking foredeep basins such as the Sonoma orogen of the western U.S. Cordillera may develop as a result of localized contraction over deep-seated weaknesses within the lithosphere. The half-width of the model orogen increases with progressive shortening, consistent with the inference that deformation in many fold and thrust belts migrated away from the hinterland with time. For example, contraction in the southern Brooks Range began in Late Jurassic time (Pallister et al., 1989), whereas deformation in the foreland regions of the North Slope is active today (Oldow et al., 1987; Grantz et al., 1987; O'Sullivan et al., 1993). Similarly, deformation in the foreland of the Sevier fold and thrust belt in Utah and eastern Idaho postdates contraction in the hinterland in Nevada and western Idaho (Royse et al., 1975; Villien and Kligfield, 1986).

Model 2. Crustal Weakness

The second model examines strength heterogeneities that lie entirely within the crust. For convenience, the weakness is modeled by including a 5-km-thick sedimentary section that increases linearly in thickness over a 350-km-wide region to 17.5 km at the left edge of the model. This weakens the middle crust, reducing the strength of the lithosphere by up to 22% (Fig. 7). The symmetry boundary condition applies to the left side of the model, so strictly speaking this model may be analogous to the right half of a symmetric cratonic sedimentary basin. However, we believe the model results are representative of deformation in regions encompassing crustal weaknesses, which may result from a variety of causes. In contrast to model 1, horizontal strain is less widely distributed at midcrustal and shallower depths than at the base of the crust (Figs. 8A through 8C). This is intuitive, given that the weakness lies within the middle and upper crust, rather than in the upper mantle as in the previous model. Pure shear thickening of the upper crust (Fig. 7) is accommodated by development of a subhorizontal shear zone at the base of the weak sedimentary layer which decouples strain in the upper crust from the lower crust. At any given time, the magnitude and horizontal distribution of strain are similar at all levels in the upper crust beneath the orogen. In the underlying crystalline crust, the magnitude of maximum strain decreases downward as strain becomes distributed over a wider area (Fig. 8C). At all depths, high strain accumulation is restricted to the width of the region encompassing the weakened portion of the lithosphere, with the locus of highest strain lying near the weakest point. As in model 1, a small amount of strain is transmitted into the unweakened portion of the lithosphere. The model demonstrates the first-order vertical strain partitioning seen in seismic reflection profiles across many fold and thrust belts, where relatively undeformed crystalline basement underlies an imbricated sedimentary sequence (e.g., Bally et al., 1966; Cook et al., 1979; Potter et al., 1986; Luetgert et al., 1987; Pratt et al., 1988; Sheridan et al., 1991).

Topography in model 2 differs markedly from model 1. Uplift occurs over a much narrower region, and most of it is confined to within the weakened region (Fig. 8D). The topographic slope continentward of the highest elevations (to the right in Fig. 8D) increases with increasing shortening and maximum elevation. The increase in topographic slope during contraction is unlike the growth of a homogeneous critically tapered wedge, suggesting that orogen evolution is strongly influenced by mechanical heterogeneities at midcrustal or shallower depths. In this model most of the crustal thickening occurs by pure shear at shallow depths, creating a topographic load that leads to subsidence and formation of a foreland basin straddling the boundary between weakened and unweakened crust (Fig. 8D).

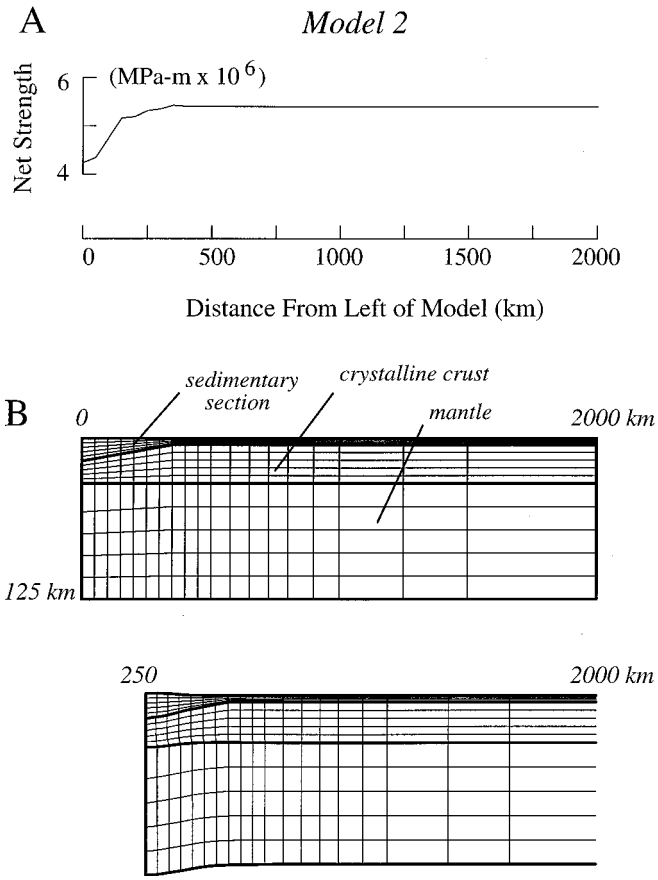

Figure 7. Model 2 (midcrustal weakness); structural evolution. The lithosphere is weakened by an increase in the thickness of the sedimentary section from 5 km to 17.5 km over a 350-km-wide region at the left side of the model. (A) Lateral variation in strength, determined as in Figure 5. (B) Finite element mesh prior to contraction and after 250 km of shortening. The model is 5000 km wide prior to contraction, but only the first 2000 km are shown. Heavy lines indicate lithologic boundaries. Vertical exaggeration is 5:1.

Model 3. Strong/Weak Crustal Boundary

Model 3 examines the case in which a relatively strong crust impinges upon weaker crust (Figs. 9 and 10). The weak crust is modeled with a 17.5-km-thick sedimentary section overlying crystalline basement, whereas the strong crust is modeled with a 5-km-thick sedimentary section. The two crustal provinces are separated by a 350-km-wide transition zone in which the thickness of the sedimentary section increases linearly at the expense of the crystalline crust (Fig. 9). The model is conceptually similar to a transition from the cratonic interior to an asymmetric sedimentary basin, but the

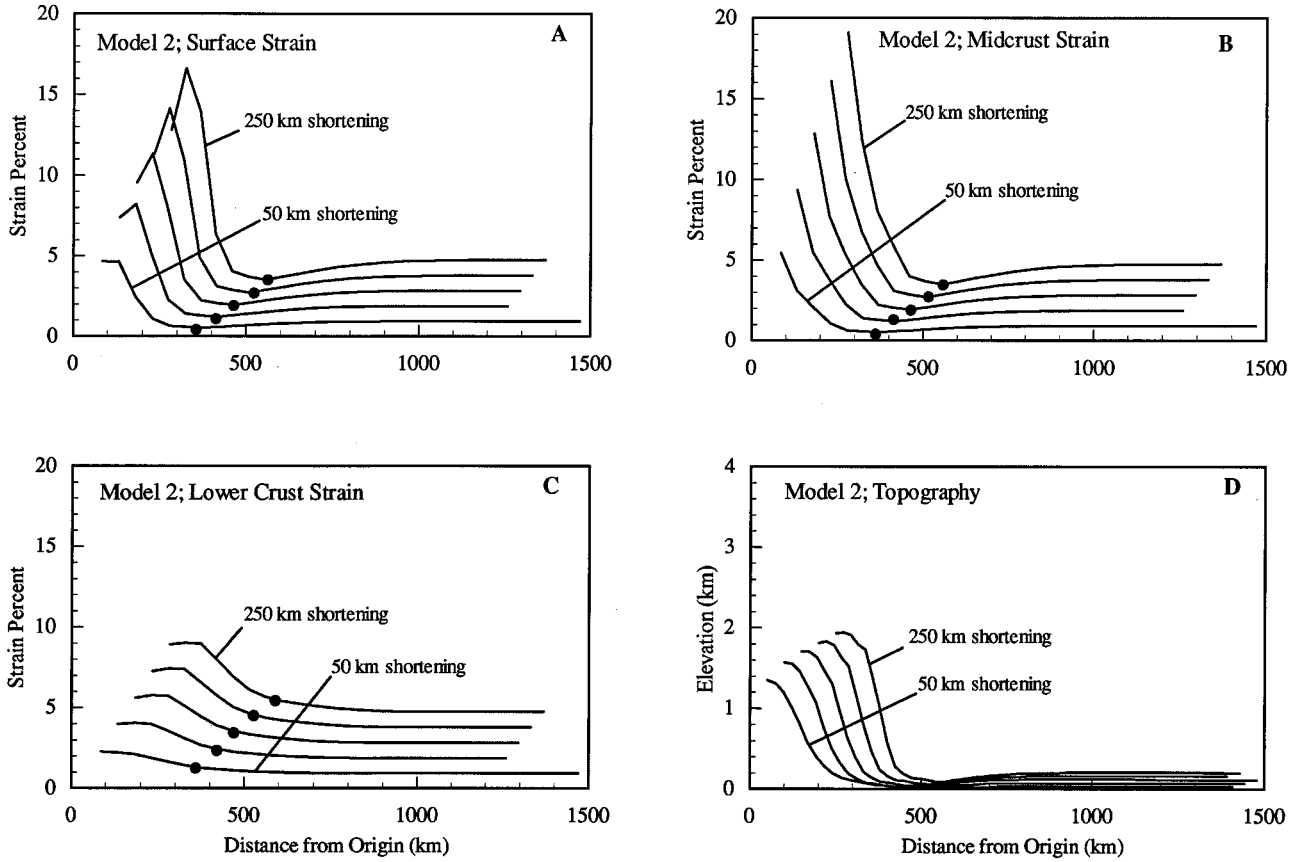

Figure 8. Model 2 (midcrustal weakness); elevation and horizontal strain. Solid circles indicate the position where the sedimentary section begins to thicken toward the left. High strain is confined to within the region encompassing the weakness at all levels in the crust. (A) Surface strain is more strongly focused and is of greater intensity than in model 1. (B) The distribution of strain at the base of the sedimentary section is similar to the surface. (C) Strain at the base of the crust is more diffuse than in the upper crust. (D) Topography is much more pronounced than in model 1 and increases in slope during the first 100 km of shortening.

behavior of the model is considered to be representative of deformation in regions where two crustal provinces of differing strength are in proximity. Each side of the model lies approximately 750 km away from the transition region, so deformation in the model is not influenced by the zero shear stress boundary condition at the edges of the model.

As in model 2, strain is most strongly localized at midcrustal depths where the rheologic differences in the lithosphere are most pronounced (Fig. 10). Strain at the surface is more broadly distributed, with high strain extending in either direction into both the weak crust with the thick sedimentary section and crust with transitional sediment thickness (Fig. 10A). The greatest strain in the middle crust is centered over the contact between the strong crust (containing the thin sedimentary section) and crust with transitional sediment thickness (Fig. 10B). The more focused nature of strain in the middle crust means that midcrustal rocks on either side of this position are moving toward the interior of the orogen relative to the overlying upper crust. This creates oppositely facing displacement directions which are accommodated by shear at the base of the sedimentary section. Shear stress transmitted across the low-angle detachments induces deformation in the upper crust, creating regions of high strain accumulation both to the left and right of the center of the region of high strain in the middle crust (Fig. 10A). At the center of the high strain region in the middle crust there is no relative displacement between the upper crust and middle crust, and a region of relatively low strain develops in the upper crust above this position in the interior of the orogen.

The portion of the lithosphere containing the thick sedimentary section lies ~1 km higher than the adjacent regions prior to contraction due to isostatic compensation of the great thickness of low-density sediments (Fig. 10D). During contraction a broad topographic high develops over the contact between the weak crust on the right of the model and the transitional crust. The topographic slope in the region to the right of the highest elevation increases slightly during the first 100 km of shortening. With further contraction the slope remains relatively constant, similar to the behavior of a homogeneous critically tapered wedge.

Model 4. Strong Oceanic Lithosphere Impinging on an Embedded Crustal Weakness

This model examines the manner in which the various types of mechanical heterogeneities discussed above interact during orogenesis. We focus in particular on the case in which contraction occurs along a previously rifted continental margin. Examples of such orogens include the Ouachita orogen, the southern Appala-

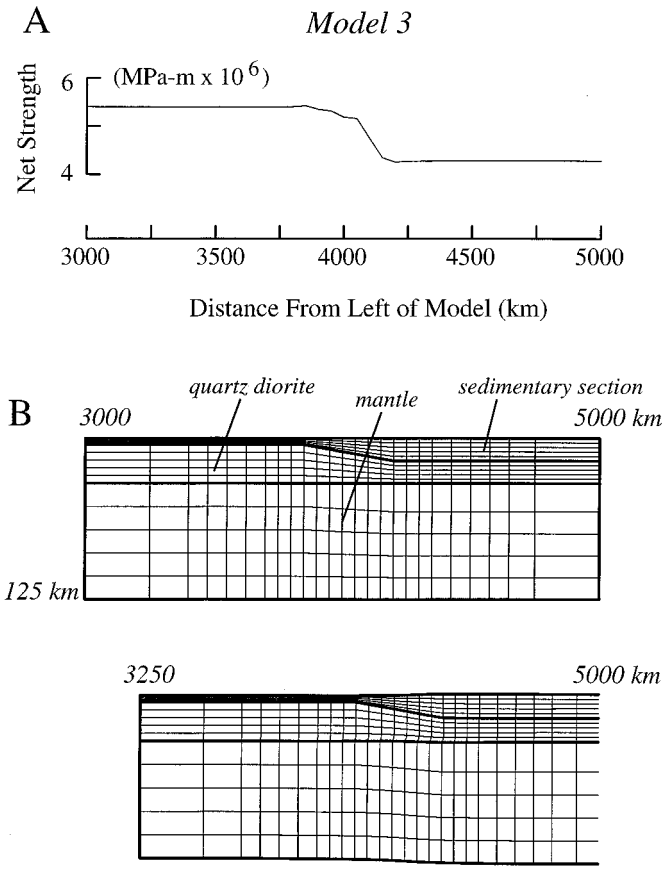

Figure 9. Model 3 (strong and weak crust boundary); structural evolution. The upper crust on the right side of the model is weakened by increasing the thickness of the sedimentary section from 5 km to 17.5 km. (A) Lateral variation in strength, determined as in Figure 5. (B) Finite element mesh prior to contraction and after 250 km of shortening. The model is initially 8000 km wide, but only the central 2000 km are shown. Heavy lines indicate lithologic boundaries. Vertical exaggeration is 5:1.

chians, the Mesozoic western North American Cordillera, and the Brooks Range of Arctic Alaska (Oldow et al., 1989; Rankin et al., 1989; Viele and Thomas, 1989). Major features of the model include a strong oceanic lithosphere on the left, a weaker continental lithosphere on the right, and a thick sedimentary section near the ocean/continent transition (Fig. 11). The oceanic lithosphere consists of a 5-km-thick gabbroic crust overlain by a 2.5-km-thick sedimentary section. The continental lithosphere consists of 5-km-thick sedimentary section overlying a 30-km-thick dioritic crystalline crust. The sediments thicken over a 350-km-wide region at the continental margin, reaching a maximum thickness of 17.5 km. Both the sedimentary section and the crystalline crust thin to oceanic thicknesses over an additional 150 km. This geometry is typical of many mature rifted continental margins such as the United States Atlantic and Gulf of Mexico margins and is thought to be representative of continental margins present prior to contraction at many orogens (i.e., the Ouachita and Appalachian orogens). The portion of the model in which the sedimentary section thickens seaward at the expense of the crystalline crust is analogous to the proximal shelf and the region in which the net thickness of the continental crust decreases seaward is analogous to the distal shelf and continental slope. The juxtaposition of strong oceanic lithosphere against relatively weak continental lithosphere creates a lateral strength heterogeneity similar to that of model 3. The thick sedimentary sequence on the continental shelf creates an embedded weakness in the middle crust (models 2 and 3), which straddles a broader strength heterogeneity in the upper mantle (model 1) where the crust thins and the upper-mantle strong layer thickens.

In the oceanic portion of the model most of the compressive stress is supported in the upper mantle (Fig. 12A[1]). This layer of high stress bifurcates beneath the continental margin and separates into layers of high stress in the upper mantle and middle crust separated by a low stress layer in the weak lower crust within the continental interior. This bifurcation is a result of the stratified rheology of the continental lithosphere (Fig. 4). During the early stages of contraction the high stress layer in the middle crust dips seaward beneath the continental margin, where the oceanic and continental stress regimes join (Fig. 12A). Examination of the strain rate in the model reveals that the strong oceanic lithosphere behaves as a relatively rigid indenter into the weaker continental lithosphere (Fig. 12B). The mantle beneath the thinned continental crust near the ocean/continent transition also undergoes little strain during the early stages of contraction and underthrusts the seaward edge of the continental crust. Underthrusting is accommodated along a basal decollement that develops on the seaward side of the orogen in the weak layer in the lower crust. This detachment is marked by a thin layer deforming at a high rate of high strain (Fig. 12B). This shear zone extends beneath the entire width of the orogen and far continentward of the loci crustal shortening. Shear stress along this detachment produces contraction and crustal thickening throughout the lower crust in this region, with the greatest strain rates occurring directly above the position at which the mantle begins to shoal. A second shear zone develops within the orogen at the base of the weak sedimentary section in the middle crust, partially decoupling strain in the lower crust from strain within the upper crust. The lower crust is underthrusting the upper crust in this region, creating shear stress along the detachment, which in combination with convergence of the oceanic crust results in pure shear shortening and crustal thickening in the upper crust within the orogen. Deformation at midcrustal and shallower depths on the seaward side of the orogen is concentrated where the midcrustal shear zone is straining most rapidly (Fig. 12B) and lies seaward of the locus of most intense deformation in the lower crust. This region of rapid strain in the upper crust is coincident with the position at which the layer supporting high compressive stress in the mantle bifurcates (Fig. 12A). The midcrustal shear zone extends beneath the continentward side of the orogen, producing a doubly vergent geometry (e.g., Willett et al., 1993; Beaumont and Quinlan, 1994). Deformation in the upper crust on the continentward side of the orogen is driven by shear along the midcrustal detachment and is less rapid and more broadly distributed than on the seaward side of the orogen. The midcrustal detachment dies out toward the continental interior, and no relative displacement occurs between the two crustal layers beyond this point. With no basal shear to drive deformation in the middle and upper crust, deformation ceases. The continentward edge of the

[1]Data Repository item 9555, color copies of Figures 12A through 12F, is available on request from Documents Secretary, GSA, P.O. Box 9140, Boulder, CO 80301.

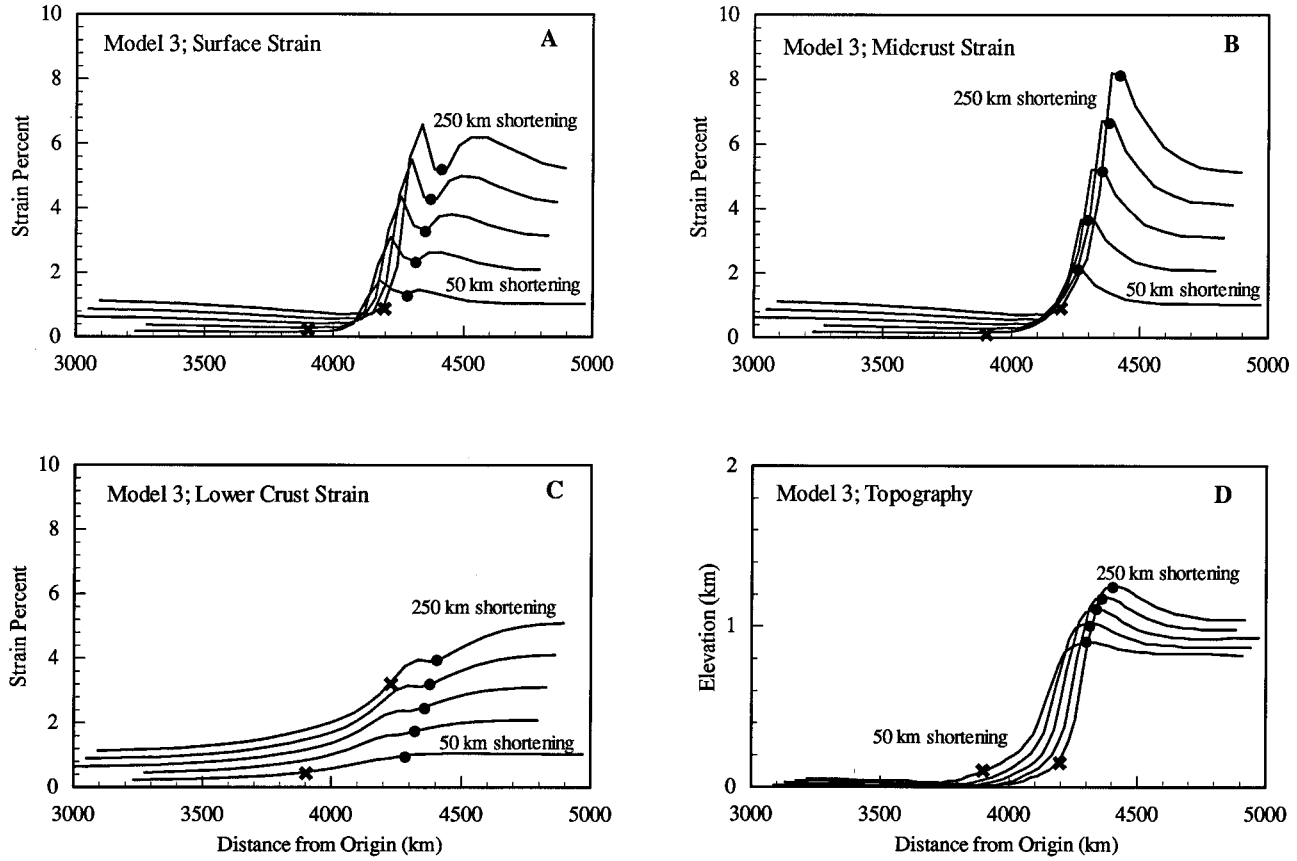

Figure 10. Model 3 (strong and weak crust boundary); elevation and horizontal strain. Crosses indicate the contact between crust with a thin sedimentary section and crust with transitional sedimentary rock thickness. Solid circles indicate the contact between transitional crust and crust with thick sedimentary section. (A) Surface strain is diffuse and extends into unweakened crust where the sedimentary section is thinnest. The highest surface strain occurs above the contact between the transitional crust and unweakened crust. A region of relatively low strain develops to the right of this position. (B) Strain at the base of the sedimentary section is more strongly focused than at the surface, with the greatest strain displaced to the right relative to the locus of highest surface strain. (C) Strain at the base of the crust is diffusely distributed across the boundary. (D) The topographic expression of the orogen is focused over the contact between crust with thick sedimentary rocks and transitional crust. Note that the lithosphere with the thicker sedimentary section is initially 1 km higher than the adjacent crust.

orogen is thus marked by the landward extent of the midcrustal shear zone.

With continued contraction the midcrustal shear zone begins to widen, expanding toward the continental interior (Figs. 12D and 12F). As a result, deformation in the upper crust begins to propagate toward the continent, and strain rate in the upper crust in the central part of the orogen decreases. Deformation is restricted to shallow levels at the leading edge of the orogen. This behavior is typical of propagation of foreland fold and thrust belts observed in many orogens such as the Brooks Range and Sevier belt (see discussion of model 1). The highest rate of strain in the lower crust remains focused beneath the central orogen during this period. Stress levels in the deep crust beneath the central orogen (Figs. 12C and 12E) decrease to the point where the upper part of the lower crust no longer supports large compressive stress after about 250 km of shortening. Instead, the two-layer pattern of stress concentration in the continental interior extends to the seaward edge of the orogen. Stress is transmitted through the central orogen and into the foreland on the continentward side via the midcrustal stress guide.

The shear zones in the middle and lower crust partition deformation into distinct shallow crustal, deep crustal, and mantle strain domains. Comparison of accumulated horizontal strain at different levels shows that the magnitude and spatial distribution of strain varies little within the interior of each strain domain, but the pattern of strain differs between domains (Fig. 13). For example, after 250 km of shortening the pattern of strain at the surface in the region between 900 km and 1200 km is similar to that at the base of the sedimentary section (Figs. 13A and 13B). The pattern of strain at the top of the crystalline crust in this region (Fig. 13C) differs from that of the sedimentary section (note especially the location of maximum strain) but is similar to that observed at the base of the crust (Fig. 13D). Strain at the leading edge of the orogen on the continentward side increases at a greater rate than strain in the interior of the orogen (Fig. 13), indicating that propagation of deformation toward the continental interior is accompanied by a shift in the locus of strain from the central interior of the orogen to the continentward side of the orogen. A region of relatively low accumulated horizontal strain develops between the interior of the orogen and the con-

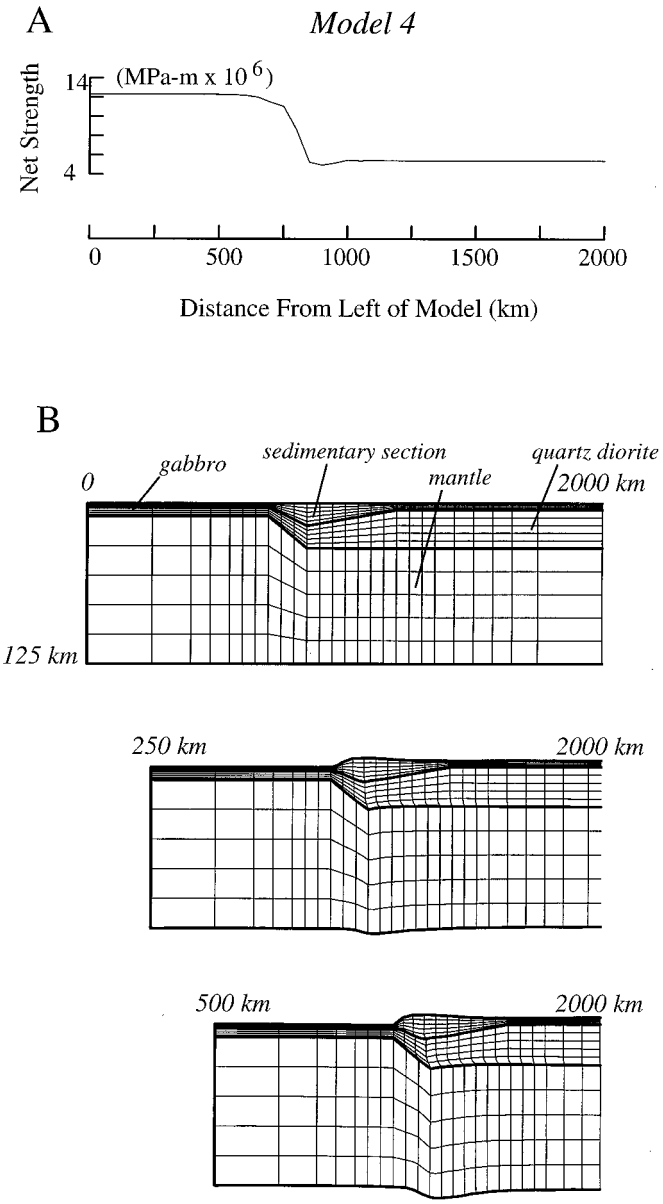

Figure 11. Model 4 (passive continental margin); structural evolution. The passive margin is the weakest part of the model due to the thick sedimentary section and is bounded by strong oceanic lithosphere on the left and relatively weak continental lithosphere on the right. (A) Lateral variation in strength, determined as in Figure 5. (B) Finite element mesh prior to contraction, after 250 km of shortening, and after 500 km of shortening. The model is initially 8000 km wide, but only the first 2000 km are shown. Heavy lines indicate lithologic boundaries. Vertical exaggeration is 5:1.

tinentward leading edge, which is similar to that described in model 3. The decrease in the rate of strain accumulation in this region indicates diminishing deformation in the interior of the orogen after about 250 km of shortening as deformation shifts to the propagating continentward foreland. The region of relatively high strain that develops in the upper crust in the foreland region (Figs. 13A and 13B; located at 1150 km and 1400 km after 250 km and 500 km of shortening, respectively) is located roughly 50 km farther toward the continental interior than the locus of greatest strain in the lower crust (Figs. 13C and 13D; located at 1100 km and 1350 km after 250 km and 500 km of shortening, respectively). Thus, strain in the region undergoing newly developed shallow deformation does not extend to midcrustal depths and is consistent with propagating thin-skinned deformation in foreland regions of orogenic belts.

The topographic slope in the model continentward of the highest elevations increases rapidly during the first 100–150 km of shortening (Fig. 14), in contrast to the pattern predicted by homogeneous critically tapered wedge models for foreland deformation. As in models 2 and 3, this suggests that preexisting heterogeneities play a key role in determining the morphological evolution of orogens during the early stages of shortening. After about 150–200 km of shortening, however, this region maintains a fairly constant topographic slope, similar to the behavior of a critically tapered wedge. The similarity to critically tapered wedge evolution after 250 km of shortening indicates that the balance between gravitational forces, rock strength, and shear stress along the midcrustal detachment becomes the dominant factor controlling topography after a finite amount of shortening and preexisting heterogeneities become less significant. This transition is not surprising considering that gravitational stress within the orogen and normal stress on the basal detachment increase as the crust thickens.

In the sedimentary section the greatest accumulated horizontal strain is focused just oceanward of the thickest sedimentary rocks after 500 km of shortening (Figs. 13A and 13B). This position represents a compromise between the tendency to focus strain at the ocean continent boundary where strong oceanic crust abuts weaker continental crust (compare to model 3) and the tendency to focus strain directly above the thickest sedimentary section where the middle crust is weakest (compare to model 2). At the base of the crust, deformation is most intense where the crust-mantle boundary begins to rise (Figs. 13C and 13D). As a consequence of this offset between the loci of maximum strain in the upper and lower crust, crustal and mantle roots that develop during contraction become displaced toward the continental interior relative to the site of most intense surface deformation (Figs. 11 and 13). The dense mantle root partially balances the buoyant crustal root so that the thickest crust does not lie beneath the greatest elevation (Fig. 14). A similar horizontal offset between the highest topography and the position of the crustal root has been inferred in the European Alps (Viel et al., 1991) and the Brooks Range in Alaska (Levander et al., 1994). The decrease in crustal thickness toward the hinterland observed in many old orogens such as the Appalachians, Variscides, and western North American Cordillera (Cook, 1984; Potter et al., 1986; Luetgert et al., 1987; Pratt et al., 1988; Bois, 1991; Yoos et al., 1991) has previously been interpreted as a result of postorogenic extensional collapse (Dewey, 1988; Nelson, 1992). This model raises the possibility that such variations in crustal thickness to some degree may be primary orogenic features unrelated to postcontractional deformation.

DISCUSSION

The models presented here focus on the first-order effects of mechanical heterogeneities on the evolution of orogenic belts. Each of the three styles of heterogeneity studied were designed to create geologically reasonable lateral variations in the strength of the lithosphere. Models using heterogeneities with less pronounced strength contrasts deform similarly to models 1–4, but the effects of

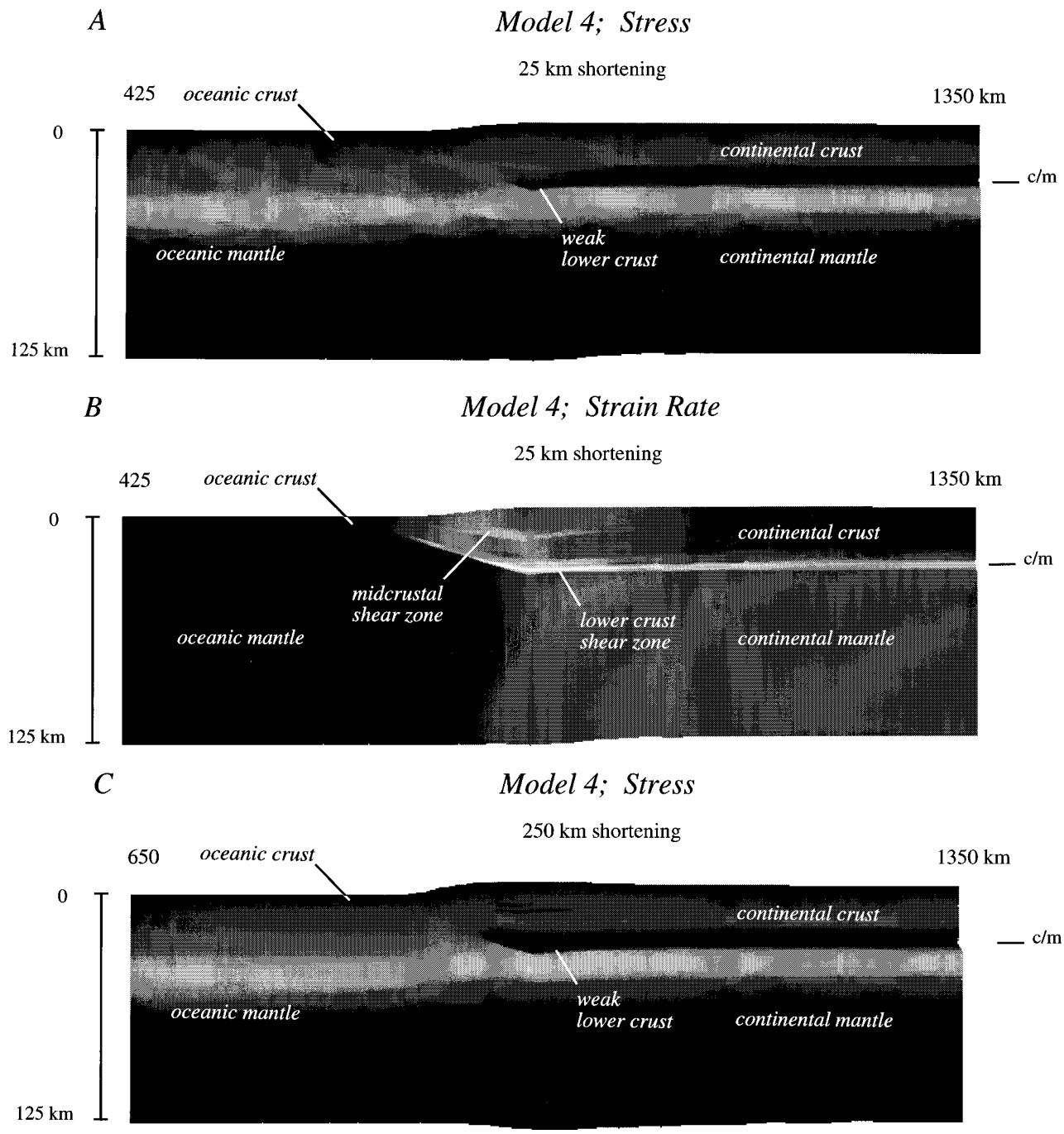

Figure 12. Model 4 (passive continental margin); second invariant of the strain rate and stress within the model lithosphere after 25 km, 250 km, and 500 km of shortening. Only the central portion of the model is shown. The horizontal coordinates indicate positions relative to the mesh diagrams in Figure 11. The gray scale represents strain rates from 10^{-14} s^{-1} to 10^{-11} s^{-1} and stress from 0 to 400 MPa, with white indicating the highest value and black indicating the lowest. The crust/mantle boundary beneath the continental interior is indicated at the right (c/m). Vertical exaggeration is 2:1. Color images of Figures 12A through 12F can be viewed on the Internet with a World Wide Web (WWW) browser at

http://zephyr.rice.edu/department/faculty/sawyer/sawyer.html

The features discussed in the text are greatly enhanced in the color images. Color copies are also available from the GSA Data Repository (see footnote 1).

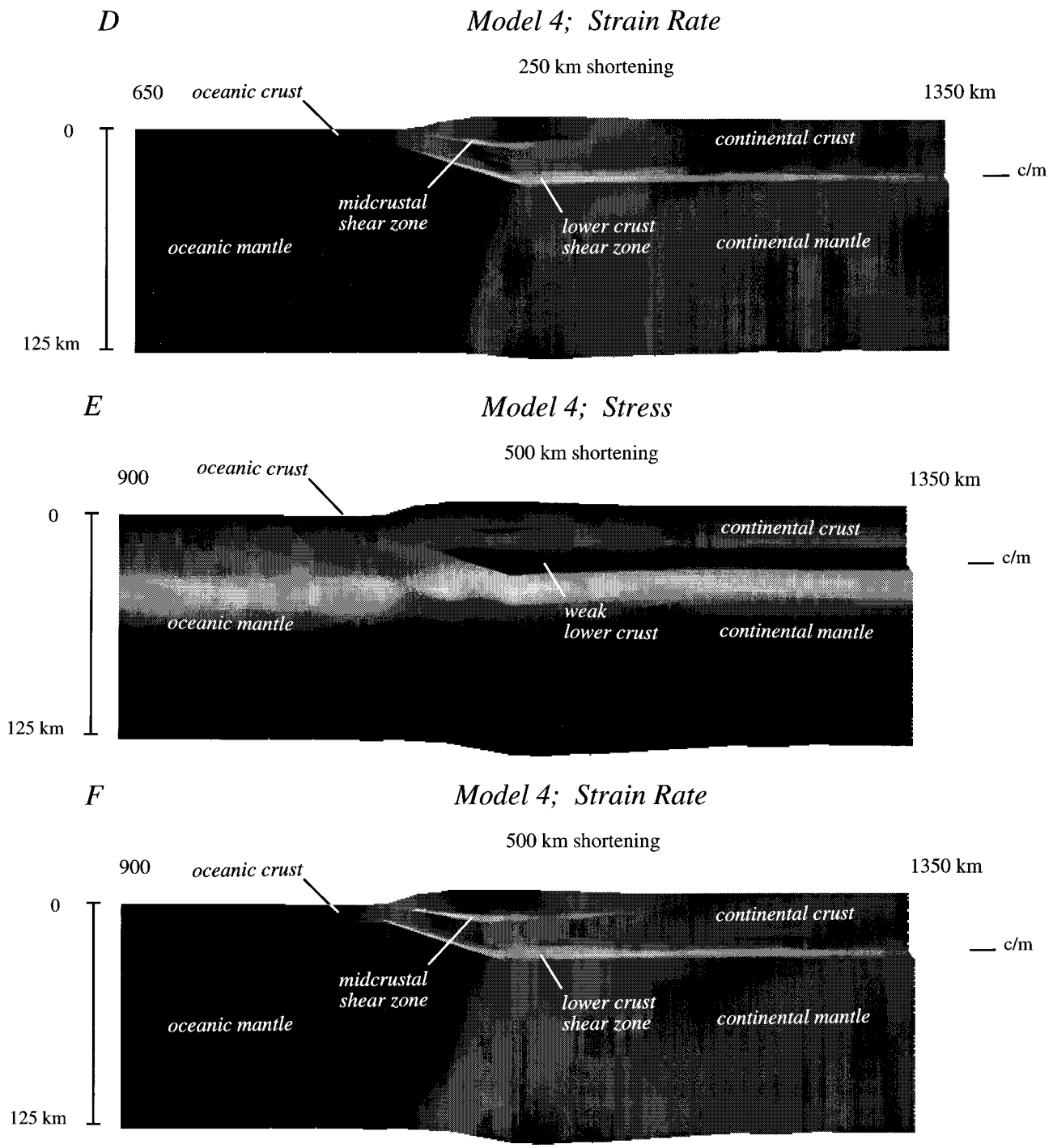

Figure 12. (*Continued*).

the heterogeneity on orogenesis are more subdued. For example, several models were run to examine the effect of sedimentary basins shallower than the 17.5 km used in model 4. The pattern of strain in these models is similar to model 4 (Fig. 13); high strain is focused in a narrow region in the upper crust, which is laterally offset from the locus of highest strain in the lower crust. However, in models with thinner sedimentary sections the focusing effect is less pronounced and strain is more evenly distributed. In general, the outer portions of the orogen in models with less pronounced strength heterogeneities approaches behavior similar to a homogeneous critically tapered wedge after less shortening than in models with more drastic lateral variations in strength.

The results of the models indicate that preexisting mechanical heterogeneities play a key role in determining how stress and strain are distributed during the early stages of orogeny. Because weak layers in the middle and lower crust decouple strain in the upper

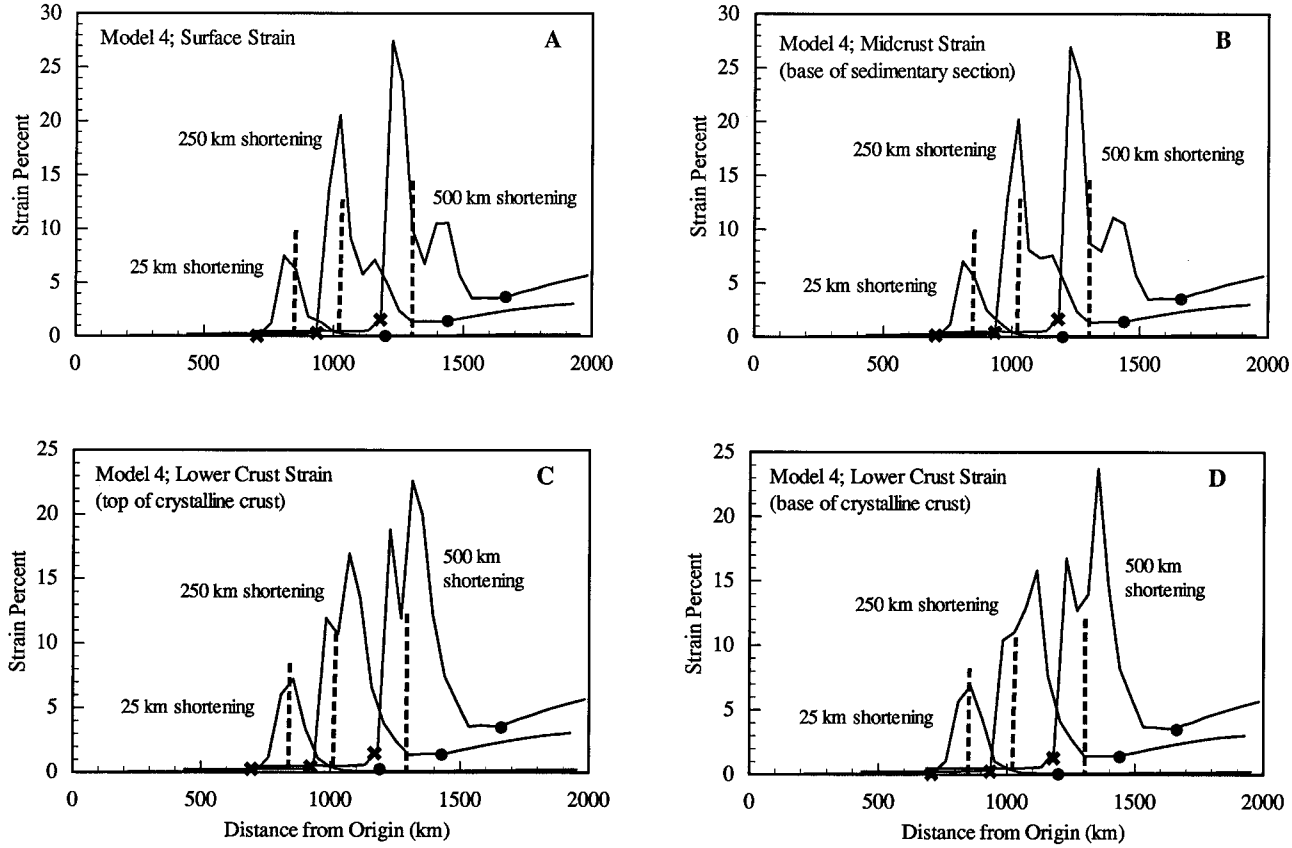

Figure 13. Model 4 (passive continental margin); horizontal strain. Symbols indicate the ocean/continent boundary (crosses) and the right edge of the sedimentary basin (solid circles). Vertical lines indicate the position of the thickest sedimentary section. (A) Surface strain is strongly focused above a point lying between the thickest sedimentary rocks and the ocean continent boundary. A secondary region of high surface strain develops closer to the continental interior with increasing shortening. (B) The pattern of strain at the base of the sedimentary section is similar to the surface. (C) Strain at the top of the crystalline basement is more broadly distributed than in the upper crust, and the locus of most intense strain is displaced continentward relative to the surface. (D) The pattern of strain at the base of the crust is similar to the top of the crystalline basement. During the first 25 km of shortening, strain is distributed similarly at all depths in the crust.

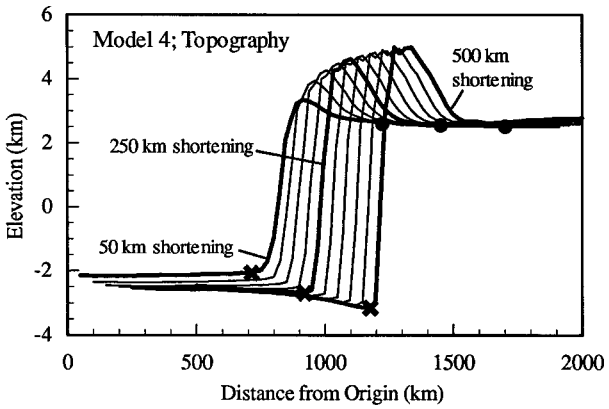

Figure 14. Model 4 (passive continental margin); elevation. Symbols indicate the ocean/continent boundary (crosses) and the right edge of the sedimentary basin (solid circles). Vertical lines indicate the position of the thickest sedimentary section. The surface expression of the orogen develops over the position where the sedimentary section begins to thicken oceanward.

crust, lower crust, and mantle, deformation is most strongly focused at the depth where lateral variations in strength are most pronounced and is more diffusely distributed at other depths. As a result, different types of heterogeneities produce characteristic patterns of deformation. (1) Deep-seated heterogeneities such as those produced by variations in crustal thickness impact the strength of the lithosphere most strongly in the uppermost mantle, focusing strain in a narrow region in the lower crust (model 1). Surface deformation and uplift are broadly distributed, with the intensity of surface strain decreasing monotonically to either side of the heterogeneity. Well-developed foreland basins are lacking. (2) Weaknesses in the upper crust such as those produced by thick sedimentary sections reduce the strength of the middle and upper crust, resulting in strongly localized deformation at the surface, more diffuse deformation at the base of the crust, and formation of a well-developed foreland basin (model 2). (3) In areas in which strong crust abuts weaker crust, deformation is strongly localized near the surface and is most intense in the transitional region separating the two types of crust (model 3).

The structural style of the orogen at the surface is strongly affected by mechanical heterogeneities in the middle and upper crust. These heterogeneities are most important during the early stages of contraction, during which time the morphologic evolution of the orogen differs significantly from a critically tapered wedge. After a moderate amount of shortening (ca. 150 km), sufficient crustal thickening develops for the balance between gravitational forces and basal shear to become dominant. The morphology of the foreland thereafter grows in a manner similar to that of a critically tapered wedge (e.g., Dahlen, 1984).

A fundamental feature of the models is the development of narrow low-angle shear zones in the middle and lower crust. These shear zones decouple deformation at different levels, partitioning strain into upper crustal, lower crustal, and mantle strain domains. The style of strain is uniform within the interior of each domain but differs markedly between domains. The shear zones develop during the earliest stages of contraction and extend throughout the entire width of the orogen. This vertical strain partitioning is compatible with the model of Oldow et al. (1990), who suggested that deformation within the crust is decoupled from the deeper lithosphere by a basal decollement extending beneath the entire orogen. The models presented here suggest several decollements provide successively further degrees of strain decoupling with increasing depth.

Vertical strain partitioning has a major impact on the horizontal pattern of strain distribution within the interior of the model orogen. The horizontal extent of deformation in fold and thrust belts has been shown to be inversely proportional to the weight (or thickness) of the deforming layer and the shear stress on the underlying decollement (cf. Hubbert and Rubey, 1959; Elliot, 1976). The midcrustal shear zone in the models decouples the upper crust from the deeper portions of the orogen, allowing it to behave as a relatively thin coherent sheet moving on a weak decollement. As a consequence, deformation is distributed over a relatively wide area incorporating both the hinterland and foreland regions. The crystalline crust is also underlain by a relatively weak basal decollement, but it bears the weight of the entire crustal section. The weight of the overlying crust results in a large normal stress on the decollement and hence requires large shear stress to produce slip in a manner analogous to frictional fault sliding. Consequently, intense contractional deformation at lower crustal depths is restricted to a relatively narrow region within the hinterland.

The shear zone in the lower crust extends more than 500 km continentward of the orogen (Fig. 12). The resulting basal shear produces a small amount of crustal strain at great distances beyond the frontal fold and thrust belt. In the model examined here, this region undergoes up to 5%–10% of strain (Fig. 13). This is similar to the amount of strain estimated in the Cumberland Plateau, well beyond the frontal part of the Appalachian fold and thrust belt (Engelder and Engelder, 1977; Engelder, 1979). The geometry depicted in the model is also similar to that described by Oldow et al. (1989) in attributing Laramide deformation in the western United States to transmission of strain over similarly great distances. Finally, mechanically twinned calcite fabrics in carbonate rocks within the North American continental interior have been interpreted to indicate up to 6% strain as far as 2100 km beyond the Ouachita and Appalachian thrust fronts (Craddock et al., 1993).

A final aspect of the models concerns temporal variations in the pattern of strain. During the earliest stages of contraction, deformation is focused within the interior of the orogen and encompasses the entire crustal column. As deformation propagates landward, thin-skinned deformation develops in the foreland region and deformation in the upper crust within the interior of the orogen wanes. This shifting pattern of deformation results in a difference in the horizontal positions of the loci of contraction in the upper crust and lower crust after 100 to 150 km of shortening (Figs. 12A and 12B). Thereafter, the locus of most intense crustal thickening lies continentward of the highest elevations and the locus of most intense surface deformation. A similar feature develops in the physical models of Shemenda (1993), which simulate convergence of buoyant lithospheric plates. These results suggest that the decrease in crustal thickness from the foreland toward the hinterland observed in many marginal orogens is not necessarily a sole consequence of postorogenic collapse. Rather, the diminished crustal thickness in the internides may develop in part during contractional deformation as a consequence of shifting loci of deformation within the orogen.

SUMMARY

Several fundamental aspects of contractional orogenesis are suggested on the basis of the modeling studies. First, deformation in orogenic belts is strongly affected by preexisting mechanical heterogeneities in the crust. Mechanical heterogeneities become less important with progressive shortening and crustal thickening and, after about 150 km of shortening, the balance between regional compressive stress and gravitational stress becomes the dominant factor controlling the orogens morphology. Second, the distribution of deformation at the surface is related to the depth at which major horizontal strength variations occur. Mechanical heterogeneities at midcrustal and shallower depths result in strongly focused surface deformation, whereas deep crustal and upper mantle heterogeneities lead to diffuse surface deformation. Third, narrow low-angle shear zones in the middle crust and lower result in vertical partitioning of strain into upper crustal and lower crustal strain domains. The upper crustal domain is characterized by diffuse deformation that migrates toward the foreland with time, accompanied by diminishing contraction in the hinterland. The lower crustal domain is characterized by more intense deformation in a narrower region and may be horizontally displaced from the locus of most intense contraction at the surface. The loci of most intense deformation in the upper crust and lower crust is controlled by the relative strength and shear strain rate on the midcrustal and lower crustal shear zones, respectively.

ACKNOWLEDGMENTS

We thank Chris Beaumont and Raymond Price for their helpful reviews, and Neville Carter, Paul Stoddard, and Anthony Gangi for their comments on an earlier version of the manuscript.

REFERENCES CITED

Allmendinger, R. W., Figueroa, D., Snyder, D., Beer, J., Mpodozis, C., and Isacks, B. L., 1990, Foreland shortening and crustal balancing in the Andes at 30°S latitude: Tectonics, v. 9, p. 789–809.

Bally, A. W., 1981, Thoughts on the tectonics of folded belts, *in* McClay, K. R., and Price, N. J., eds., Thrust and nappe tectonics: Geological Society of London Special Publication 9, p. 13–32.

Bally, A. W., Gordy, P. L., and Stewart, C. A., 1966, Structure, seismic data and orogenic evolution of the southern Canadian Rockies: Canadian Society of Petroleum Geologists Bulletin, v. 14, p. 337–381.

Barr, T. D., and Dahlen, F. A., 1989, Brittle frictional mountain building, 2. Thermal structure and heat budget: Journal of Geophysical Research, v. 94, p. 3923–3947.

Barr, T. E., Dahlen, F. A., and McPhail, D. C., 1991, Brittle frictional mountain building, 3. Low-grade metamorphism: Journal of Geophysical Research, v. 96, p. 10319–10338.

Beaumont, C., and Quinlan, G., 1994, A geodynamic framework for interpreting crustal-scale seismic-reflectivity patterns in compressional orogens: Geophysical Journal International, v. 116, p. 754–783.

Bois, C., 1991, Geologic significance of seismic reflections in collision belts: Geophysical Journal International, v. 105, p. 55–69.
Bott, M. H. P., 1990, Stress distribution and plate boundary force associated with collision mountain ranges: Tectonophysics, v. 182, p. 193–209.
Braun, J., 1993, Three-dimensional numerical modeling of compressional orogenies: Thrust geometry and oblique convergence: Geology, v. 21, p. 153–156.
Byerlee, J. D., 1968, Brittle-ductile transition in rocks: Journal of Geophysical Research, v. 73, p. 4741–4750.
Byerlee, J. D., 1978, Friction in rocks: Pure and Applied Geophysics, v. 116, p. 615–626.
Carter, N. L., and Tsenn, M. C., 1987, Flow properties of continental lithosphere: Tectonophysics, v. 136, p. 27–63.
Chapple, W. M., 1978, Mechanics of thin-skinned fold-and-thrust belts: Geological Society of America Bulletin, v. 89, p. 1189–1198.
Chery, J., Villote, J. P., and Daignieres, M., 1991, Thermomechanical evolution of a thinned continental lithosphere under compression: Implications for the Pyrenees: Journal of Geophysical Research, v. 96, p. 4385–4412.
Chopra, P. N., and Paterson, M. S., 1981, The experimental deformation of dunite: Tectonophysics, v. 78, p. 453–473.
Choukroune, P., and ECORS Team, 1989, The ECORS Pyrenean deep seismic profile reflection data and the overall structure of an orogenic belt: Tectonics, v. 8, p. 23–89.
Cook, F., 1984, Geophysical anomalies along strike of the southern Appalachian piedmont: Tectonics, v. 3, p. 45–62.
Cook, F., Albaugh, D., Brown, L., Kaufman, S., Oliver, J., and Hatcher, R., Jr., 1979, Thin-skinned tectonics in the crystalline southern Appalachians: COCORP seismic reflection profiling of the Blue Ridge and Piedmont: Geology, v. 7, p. 563–567.
Cook, F. A., Varsek, J. L., and Clowes, R. M., 1991, LITHOPROBE reflection transect of southwestern Canada: Mesozoic thrust and fold belt to mid-ocean ridge, *in* Meissner, R., Brown, L., Durbaum, H.-J., Franke, W., Fuchs, K., and Seifert, F., eds., Continental lithosphere: Deep seismic reflections: American Geophysical Union Geodynamics Series, v. 22, p. 247–256.
Costain, J. K., Hatcher, R. D., Jr., Çoruh, C., Pratt, T. L., Taylor, S. R., Litehiser, J. J., and Zietz, I., 1989, Geophysical characteristics of the Appalachian crust, *in* Hatcher, R. D., Jr., Thomas, W. A., and Viele, G. W., eds., The Appalachian-Ouachita orogen in the United States: Boulder, Colorado, Geological Society of America, Geology of North America, v. F-2, p. 385–416.
Craddock, J. P., Jackson, M., van der Pluijm, B. A., and Versical, R. T., 1993, Regional shortening fabrics in eastern North America: Far-field stress transmission from the Appalachian-Ouachita orogenic belt: Tectonics, v. 12, p. 257–264.
Dahlen, F. A., 1984, Noncohesive critical coulomb wedges: An exact solution: Journal of Geophysical Research, v. 89, p. 10125–10133.
Dahlen, F. A., and Barr, T. E., 1989, Brittle frictional mountain building, 1. Deformation and mechanical energy budget: Journal of Geophysical Research, v. 94, p. 3906–3922.
DeBremaecker, J.-C., 1977, Is the oceanic lithosphere elastic or plastic?: Journal of Geophysical Research, v. 82, p. 2001–2004.
Dewey, J. F., 1988, Extensional collapse of orogens: Tectonics, v. 7, p. 1123–1140.
Dunbar, J. A., 1988, Kinematics and dynamics of continental breakup [Ph.D. dissert.]: Austin, Texas, University of Texas, 171 p.
Dunbar, J. A., and Sawyer, D. S., 1989, How preexisting weaknesses control the style of continental breakup: Journal of Geophysical Research, v. 94, p. 7278–7292.
Elliot, D., 1976, The energy balance and deformation mechanisms of thrust sheets: Philosophical Transactions of the Royal Society of London, Series A, v. 283, p. 289–312.
Engelder, T., 1979, Mechanisms for strain within the upper Devonian clastic sequence of the Appalachian plateau, western New York: American Journal of Science, v. 279, p. 527–542.
Engelder, T., and Engelder, R., 1977, Fossil distortion and decollement tectonics of the Appalachian plateau: Geology, v. 5, p. 457–460.
England, P., and McKenzie, D., 1982, A thin viscous sheet model for continental deformation: Geophysical Journal of the Royal Astronomical Society, v. 70, p. 295–321.
England, P., Houseman, G., and Sonder, L., 1985, Length scales for continental deformation in convergent, divergent, and strike-slip environments: Analytical and approximate solutions for a thin viscous sheet model: Journal of Geophysical Research, v. 90, p. 3551–3558.
Foster, D. A., Miller, C. F., Harrison, T. M., and Hoisch, T. D., 1992, $^{40}Ar/^{39}Ar$ thermochronology and thermobarometry of metamorphism, plutonism, and tectonic denudation in the Old Woman Mountains area, California: Geological Society of America Bulletin, v. 104, p. 176–191.
Grantz, A., Dinter, D. A., and Culotta, R. C., 1987, Structure of the continental shelf north of the Arctic National Wildlife Refuge, *in* Bird, K. J., and Magoon, L. B., eds., Petroleum geology of the northern part of the Arctic National Wildlife Refuge, northeastern Alaska: U.S. Geological Survey Bulletin 1778, p. 271–276.
Hansen, F. D., and Carter, N. L., 1982, Creep of selected crustal rocks at 1000 MPa: Eos (Transactions, American Geophysical Union), v. 63, p. 437.
Harry, D. L., and Sawyer, D. S., 1992a, A dynamic model of extension in the Baltimore Canyon trough region, U.S. Atlantic margin: Tectonics, v. 11, p. 420–436.
Harry, D. L., and Sawyer, D. S., 1992b, Basaltic volcanism, mantle plumes and the mechanics of rifting: The Parana flood basalt province of South America: Geology, v. 20, p. 207–210.
Harry, D. L., Sawyer, D. S., and Leeman, W. P., 1993, The mechanics of continental extension: Implications for the magmatic and structural evolution of the Great Basin: Earth and Planetary Science Letters, v. 117, p. 59–71.
Hatcher, R. D., and Odom, A. L., 1980, Timing of thrusting in the southern Appalachians, USA; Model for orogeny?: Journal of the Geological Society of London, v. 137, p. 321–327.
Houseman, G., and England, P., 1986, Finite strain calculations of continental deformation, 1. Method and general results for convergent zones: Journal of Geophysical Research, v. 91, p. 3651–3663.
Hubbert, M. K., and Rubey, W. W., 1959, Role of fluid pressure in mechanics of overthrust faulting. I. Mechanics of fluid-filled porous solids and its application to overthrust faulting: Geological Society of America Bulletin, v. 70, p. 115–166.
James, D. E., 1971, Plate tectonic model for the evolution of the central Andes: Geological Society of America Bulletin, v. 82, p. 3325–3346.
Laubscher, H. P., 1983, Detachment, shear, and compression in the central Alps, *in* Hatcher, R. D., ed., Contributions to the tectonics and geophysics of mountain chains: Geological Society of America Memoir 158, p. 191–211.
Lawton, T. F., and Trexler, J. H., 1991, Piggyback basin in the Sevier orogenic belt, Utah: Implications for development of the thrust wedge: Geology, v. 19, p. 827–830.
Levander, A., Fuis, G. S., Wissinger, E. S., Lutter, W. J., Oldow, J. S., and Moore, T. E., 1994, Seismic images of the Brooks Range fold and thrust belt, Arctic Alaska, from an integrated seismic reflection/refraction experiment: Tectonophysics, v. 232, p. 13–30.
Luetgert, J. H., Mann, C. E., and Klemperer, S. L., 1987, Wide-angle deep crustal reflections in the northern Appalachians: Geophysical Journal of the Royal Astronomical Society, v. 89, p. 183–188.
Matte, P., 1991, Accretionary history and crustal evolution of the Variscan belt in western Europe: Tectonophysics, v. 196, p. 309–337.
Miller, E. L., and Gans, P. B., 1989, Cretaceous crustal structure and metamorphism in the hinterland of the Sevier thrust belt, western U.S. Cordillera: Geology, v. 17, p. 57–62.
Nelson, K. D., 1992, Are crustal thickness variations in old mountain belts like the Appalachians a consequence of lithospheric delamination?: Geology, v. 20, p. 498–502.
Nicholson, C., Sorlein, C. C., Atwater, T., Crowell, J. C., and Luyendyk, B. P., 1994, Microplate capture, rotation of the western Transverse Ranges, and initiation of the San Andreas transform as a low-angle fault system: Geology, v. 22, p. 491–495.
Oldow, J. S., Seidensticker, C. M., Phelps, J. C., Julian, F. E., Gottachalk, R. R., Boler, K. W., Handschy, J. W., and Avé Lallemant, H. G., 1987, Balanced cross sections through the central Brooks Range and North Slope, Arctic Alaska: Tulsa, Oklahoma, American Association of Petroleum Geologists, 19 p.
Oldow, J. S., Bally, A. W., Avé Lallemant, H. G., and Leeman, W. P., 1989, Phanerozoic evolution of the North American Cordillera, *in* Bally, A. W., and Palmer, A. R., eds., The geology of North America: An overview: Boulder, Colorado, Geological Society of America, Geology of North America, v. A, p. 139–232.
Oldow, J. S., Bally, A. W., and Avé Lallemant, H. G., 1990, Transpression, orogenic float and lithospheric balance: Geology, v. 18, p. 991–994.
O'Sullivan, P. B., Green, P. F., Bergman, S. C., Decker, J., Duddy, I. R., Gleadow, A. J. W., and Turner, D. L., 1993, Multiple phases of Tertiary uplift and erosion in the Arctic National Wildlife Refuge, Alaska, revealed by apatite fission track analysis: American Association of Petroleum Geologists Bulletin, v. 77, p. 359–385.
Pallister, J. S., Budahn, J. R., and Murchey, B. L., 1989, Pillow basalts of the Angayucham terrane: Oceanic plateau and island crust accreted to the Brooks Range: Journal of Geophysical Research, v. 94, p. 15901–15923.
Pfiffner, O. A., Frei, W., Valasek, P., Stauble, M., Levato, L., DuBois, L., Schmid, S. M., and Smithson, S. B., 1990, Crustal shortening in the Alpine orogen: Results from deep seismic reflection profiling in the eastern Swiss Alps, Line NFP 20-East: Tectonics, v. 9, p. 1327–1355.
Potter, C., Sanford, W., Yoos, T., Prussin, E., Keach, W., Oliver, J., Kaufman, S., and Brown, L., 1986, COCORP deep seismic reflection traverse of the interior of the North American Cordillera, Washington and Idaho: Implications for Appalachian crustal structure: Tectonics, v. 5, p. 1007–1026.
Pratt, T. L., Çoruh, C., Costain, J. K., and Glover, L., 1988, A geophysical study of the Earth's crust in central Virginia; Implications for Appalachian crustal structure: Journal of Geophysical Research, v. 93, p. 6649–6667.
Ranalli, G., and Murphy, D. C., 1987, Rheological stratification of the lithosphere: Tectonophysics, v. 132, p. 281–295.
Rankin, D. W., and nine others, 1989, Pre-orogenic terranes, *in* Hatcher, R. D., Jr., Thomas, W. A., and Viele, G. W., eds., The Appalachian-Ouachita Orogen in the United States: Boulder, Colorado, Geological Society of America, Geology of North America, v. F-2, p. 7–100.
Roeder, D., 1989, South-Alpine thrusting and trans-Alpine convergence, *in* Coward, M. P., Dietrich, D., and Park, R. G., eds., Alpine tectonics: Geological Society of London Special Publication 45, p. 211–227.
Royse, F., Jr., Warner, M. A., and Reese, D. L., 1975, Thrust belt of Wyoming, Idaho, and northern Utah—Structural geometry and related problems, *in* Bolyard, D. W., ed., Symposium on deep drilling frontiers in central Rocky Mountains: Denver, Colorado, Rocky Mountain Geological Association, p. 41–54.
Sawyer, D. S., and Harry, D. L., 1991, Dynamic modeling of divergent margin formation: Application to the U.S. Atlantic margin: Marine Geology, v. 102, p. 29–42.
Schmid, S. M., Paterson, M. S., and Boland, J. N., 1977, Super-plastic flow in finegrained limestone: Tectonophysics, v. 43, p. 257–291.
Sclater, J. G., Jaupart, C., and Galson, D., 1980, The heat flow through oceanic and continental crust and the heat loss of the Earth: Reviews of Geophysics and Space Physics, v. 18, p. 269–311.
Shemenda, A. I., 1993, Subduction of the lithosphere and back arc dynamics: Insights from physical modeling: Journal of Geophysical Research, v. 98, p. 16167–16185.
Sheridan, R. E., Olsson, R. F., and Miller, J. J., 1991, Seismic reflection and gravity study of proposed Taconic suture under New Jersey coastal plain; Implications for continental growth: Geological Society of America Bulletin, v. 103, p. 402–414.
Snyder, D. B., Ramos, V. A., and Allmendinger, R. W., 1990, Thick-skinned deformation observed on deep seismic reflection profiles in western Argentina: Tectonics, v. 9, p. 773–788.
Viel, L., Berckhemer, H., and Mueller, St., 1991, Some structural features of the Alpine lithospheric root: Tectonophysics, v. 195, p. 421–436.
Viele, G. W., and Thomas, W. A., 1989, Tectonic synthesis of the Ouachita orogenic belt, *in* Hatcher, R. D., Jr., Thomas, W. A., and Viele, G. W., eds., The Appalachian-Ouachita Orogen in the United States: Boulder, Colorado, Geological Society of America, Geology of North America, v. F-2, p. 695–728.
Villien, A., and Kligfield, R. M., 1986, Thrusting and synorogenic sedimentation in central Utah, *in* Peterson, J. A., ed., Paleotectonics and sedimentation in the Rocky Mountain region, United States: American Association of Petroleum Geologists Memoir 41, p. 353–370.
Wdowonski, S., and O'Connell, R. J., 1991, Deformation of the central Andes (15°S–27°S) derived from a flow model of subduction zones: Journal of Geophysical Research, v. 96, p. 12245–12255.
Wilks, K. R., and Carter, N. L., 1990, Rheology of some lower crustal rocks: Tectonophysics, v. 182, p. 57–77.
Willett, S., Beaumont, C., and Fullsack, P., 1993, Mechanical model for the tectonics of doubly vergent compressional orogens: Geology, v. 21, p. 371–374.
Yoos, T. R., Potter, C. J., Thigpen, J. L., and Brown, L. D., 1991, The cordilleran foreland thrust belt in northwestern Montana and northern Idaho from COCORP and industry seismic reflection data: American Association of Petroleum Geologists Bulletin, v. 75, p. 1089–1106.
Zienkiewicz, O. C., and Godbole, P. N., 1975, Viscous, incompressible flow, with special reference to non-Newtonian (plastic) fluids, *in* Gallagher, R. H., Oden, J. T., Taylor, C., and Zienkiewicz, O. C., eds., Finite elements in fluids, v. 1: New York, John Wiley and Sons, p. 25–55.

Manuscript Received by the Society May 19, 1994
Revised Manuscript Received May 16, 1995
Manuscript Accepted May 23, 1995

Printed in U.S.A.